ELECTRONIC SUPPLEMENTARY INFORMATION (ESI)

Polyhedral borane-capped coinage metal nanoparticles as high-performing catalysts for 4-nitrophenol reduction

Nathaniel E. Larm, Dronareddy Madugula, Mark W. Lee,* and Gary A. Baker*

Department of Chemistry, University of Missouri–Columbia, Columbia, MO 65211 USA. E-mail:

leemw@missouri.edu

bakergar@missouri.edu

Experimental section.

Materials and reagents. All experiments were carried out using ultrapure Millipore water (18.2 MΩ cm). Gold (III) chloride trihydrate (520918; ≥99.9%), silver nitrate (204390; 99.9999%), sodium borohydride (480886; 99.99%), and 4-nitrophenol (241326; ≥99%) were purchased from Sigma-Aldrich (St. Louis, MO). Cesium decaborate ($Cs_2B_{10}H_{10}$) was prepared from bis-triethylammonium decaborate, which was prepared as described previously.[1] Briefly, 3.0 g (9.3 mmol) of bis-triethylammonium decaborate was dissolved in 50 ml of DI water. To this, a solution containing 2.85 g (19 mmol) of cesium hydroxide was added dropwise, with stirring. The volatiles were removed in vacuo and the white powder was resuspended in 25 ml of DI water, filtered, and dried in an oven at 104° C.

Characterization. UV–vis absorbance spectra were recorded on a Varian Cary 50 Bio Spectrophotometer using standard 1-cm PMMA cuvettes. Nuclear magnetic resonance (NMR) analysis was performed using a Bruker Avance-300 MHz spectrometer. For TEM analysis, 8-µL sample aliquots were deposited onto carbon-coated copper grids (Ted Pella, Inc.; 01814-F, support films, carbon type-B, 400 mesh copper grid) by drop-casting, followed by drying in open air. TEM micrographs were obtained on an FEI Tecnai (F20) microscope operated at a 200 keV. ImageJ software was used to analyze the resulting micrographs, and at least 300 particles were counted to create the corresponding size histograms.

[*closo*-$B_{10}H_{10}$]$^{2-}$-decorated gold nanoparticle synthesis. Millipore water was used throughout all syntheses and analyses. Just prior to use, 81.5 mg (0.2 mmol) of cesium decaborate ($Cs_2B_{10}H_{10}$) was added to a fresh 20-mL scintillation vial and dissolved in 20 mL of water to produce a 10 mM [*closo*-$B_{10}H_{10}$]$^{2-}$ stock solution. This [*closo*-$B_{10}H_{10}$]$^{2-}$ stock and an aqueous solution of 5.0 mM aqueous $HAuCl_4$ were diluted in seperate fresh 50-mL Falcon™ centrifuge tubes and diluted to 10 mL using water as per Table S1 to produce the desired range of reducing agent-to-gold ratios (R values). In each case the 10-mL solution of [*closo*-$B_{10}H_{10}$]$^{2-}$ was added to the 10-mL solution of Au^{3+} under vortex. Note that the final [Au] in all solutions was

0.25 mM. The formation of gold nanoparticles (AuNPs) occurred over 1 h, as evidenced by a color change in the mixture from colorless to light pink followed by wine red. UV–vis analysis was performed on these colloidal solutions after aging for 1 d, and again after aging for 3, 5, 7, and 14 d to monitor changes in the localized surface plasmon resonance (LSPR) band.

[*closo*-$B_{10}H_{10}$]$^{2-}$-decorated silver nanoparticle synthesis. [*closo*-$B_{10}H_{10}$]$^{2-}$-decorated AgNPs were synthesized in a manner similar to the above method (similar R values) using 5.0 mM aqueous $AgNO_3$ in the place of the 5.0 mM aqueous $HAuCl_4$. The formation of AgNPs occurred slowly over several hours, as evidenced by a color change in the final solutions from colorless to faint yellow, with higher R values resulting in a faster color change and a deeper yellow appearance. UV–vis analysis was performed similar to the above characterization for [*closo*-$B_{10}H_{10}$]$^{2-}$-decorated AuNPs.

[*closo*-$B_{10}H_{10}$]$^{2-}$-decorated bimetallic nanoparticle synthesis. [*closo*-$B_{10}H_{10}$]$^{2-}$-decorated bimetallic Au_xAg_{1-x}NPs were synthesized using an R value of 3.0, a final metal concentration of 0.25 mM, and *x* values of 0.1, 0.2, 0.3, 0.4, 0.5, 0.6, 0.7, 0.8, and 0.9. For each *x* value, a 10-mL solution containing 1.5 mM aqueous $Cs_2B_{10}H_{10}$ was rapidly added to a 10-mL solution consisting of aqueous dispersions of $HAuCl_4$ and $AgNO_3$ of the appropriate concentrations while mixing via vortex. The delay between the mixing of Ag^+ to Au^{3+} and the addition of [*closo*-$B_{10}H_{10}$]$^{2-}$ solution was purposefully kept short (< 5 s) to minimize formation of AgCl. Each solution rapidly turned a shade of orange or red, indicating NP ripening. UV–vis analysis was performed on the as-synthesized colloidal solutions and at various stability time-points to monitor changes in the LSPR.

Catalyzed reduction of 4-nitrophenol to 4-aminophenol. The model reduction of 4-nitrophenol (4-NP) to 4-aminophenol (4-AP) using sodium borohydride ($NaBH_4$) was used to assess the catalytic activity of the [*closo*-$B_{10}H_{10}$]$^{2-}$-decorated monometallic Au- and AgNPs and bimetallic Au_xAg_{1-x}NPs. A stock of 0.2 mM aqueous 4-NP was freshly prepared daily as needed. 37.8 mg of $NaBH_4$ and 10 mL of water were added to separate, fresh 20-mL scintillation vials which were both stored on ice. Just prior to use, this water was added to the solid $NaBH_4$ to produce a 0.1 M aqueous $NaBH_4$ stock, which was then stored on ice for use. This $NaBH_4$ solution was re-prepared as needed every 15 min or once consumed. For the analysis, 2.1 mL of 0.2 mM aqueous 4-NP stock and 0.9 mL of 0.1 M $NaBH_4$ stock (1:214 molar ratio 4-NP to $NaBH_4$) were added to a PMMA cuvette, creating a yellow solution of 4-nitrophenolate (λ_{max} = 400 nm). 84 µL of 0.25 mM NP solution was added to a cuvette cap (5 mol% metal to 4-NP) which was then placed on the cuvette and the solution was inverted 3–4 times to mix and placed in a spectrophotometer which was set to record absorbance at 400 nm every 0.15 s. There was about a 3–5 s delay between introduction of the NP solution and the start of the UV–vis analysis. The resulting apparent rate (k_{app}) was determined by finding the slope of the linear portion of a corresponding plot of $\ln(A_0/A_t)$ @ 400 nm *versus* time. To perform the recycling study, following reaction completion the cuvette was removed from the instrument, the cap was taken off, 84 µL of freshly prepared 5.0 mM aqueous 4-NP and 90 µL of 0.1 M aqueous $NaBH_4$ stock were spiked into the cap, the cap was replaced, the cuvette was shaken 3 times, and finally the cuvette was placed back in the instrument to continue measurements.

Table S1 Target concentrations of noble metal (Au^{3+} or Ag^{+}) and [*closo*-$B_{10}H_{10}]^{2-}$ for each corresponding R value. Solutions were prepared by rapid addition of 10 mL of [*closo*-$B_{10}H_{10}]^{2-}$ solution to 10 mL of metal solution under vortex as described above.

R Value	[noble metal] (mM)	[$B_{10}H_{10}^{2-}$] (mM)
0.5	0.25	0.125
1.0	0.25	0.25
3.0	0.25	0.75
5.0	0.25	1.25
10	0.25	2.5

Table S2 Tabulated catalytic results for [*closo*-$B_{10}H_{10}]^{2-}$-decorated AuNPs for 4-NP reduction, 5 mol% metal to 4-NP catalyst loading.

Aging	R value	k_{app} (s^{-1})	t_{rxn} (s)	TOF (h^{-1})
1 day	0.5	8.58 (±0.24) × 10^{-3}	339	202 (±5)
	1.0	9.62 (±1.52) × 10^{-3}	299	232 (±34)
	3.0	2.67 (±0.40) × 10^{-3}	1138	61 (±9)
	5.0	2.69 (±0.23) × 10^{-3}	1118	61 (±5)
	10.0	3.12 (±0.38) × 10^{-3}	969	71 (±8)
7 days	0.5	1.82 (±0.16) × 10^{-3}	1752	39 (±3)
	1.0	2.13 (±0.43) × 10^{-3}	1500	46 (±9)
	3.0	1.25 (±0.02) × 10^{-2}	232	294 (±4)
	5.0	1.76 (±0.07) × 10^{-3}	1719	40 (±2)
	10.0	*	*	*

* indicates the measurement was not performed due to visual detection of aggregates.

Table S3 Tabulated catalytic results for [*closo*-$B_{10}H_{10}]^{2-}$-decorated AgNPs for 4-NP reduction, 5 mol% metal to 4-NP catalyst loading.

Aging	R value	k_{app} (s^{-1})	t_{rxn} (s)	TOF (h^{-1})
1 day	0.5	2.49 (±0.08) × 10^{-1}	40	1691 (±14)
	1.0	1.47 (±0.18) × 10^{-1}	53	1291 (±29)
	3.0	9.21 (±1.77) × 10^{-2}	52	1330 (±83)
	5.0	6.58 (±0.60) × 10^{-2}	63	1095 (±76)
	10.0	5.04 (±0.64) × 10^{-2}	72	959 (±70)
7 days	0.5	1.40 (±0.12) × 10^{-1}	57	1207 (±27)
	1.0	1.46 (±0.06) × 10^{-1}	67	1015 (±9)
	3.0	1.77 (±0.07) × 10^{-1}	55	1239 (±33)
	5.0	1.63 (±0.03) × 10^{-1}	56	1228 (±5)
	10.0	1.26 (±0.08) × 10^{-1}	52	1304 (±40)

Table S4 Tabulated catalytic results for [*closo*-$B_{10}H_{10}$]$^{2-}$-decorated bimetallic Au_xAg_{1-x}NPs for 4-NP reduction, 5 mol% metal to 4-NP catalyst loading.

Aging	*x*	k_{app} (s^{-1})	t_{rxn} (s)	TOF (h^{-1})
1 day	0.9	8.47 (±0.18) × 10^{-3}	344	199 (±5)
	0.8	3.60 (±0.05) × 10^{-2}	71	967 (±4)
	0.7	1.34 (±0.14) × 10^{-1}	24	2925 (±271)
	0.6	1.90 (±0.06) × 10^{-1}	18	3894 (±18)
	0.5	1.67 (±0.01) × $10^{-!}$	20	3488 (±83)
	0.4	1.74 (±0.19) × $10^{-!}$	20	3426 (±650)
	0.3	1.92 (±0.02) × $10^{-!}$	19	3518 (±66)
	0.2	2.07 (±0.05) × 10^{-2}	18	3792 (±129)
	0.1	1.11 (±0.32) × 10^{-1}	35	1975 (±339)
7 days	0.9	4.76 (±0.37) × 10^{-2}	73	947 (±115)
	0.8	1.31 (±0.09) × 10^{-1}	25	2796 (±158)
	0.7	2.00 (±0.08) × 10^{-1}	15	4672 (±141)
	0.6	1.58 (±0.04) × 10^{-1}	20	3413 (±85)
	0.5	1.95 (±0.03) × $10^{-!}$	21	3208 (±261)
	0.4	1.53 (±0.03) × $10^{-!}$	23	2945 (±122)
	0.3	1.18 (±0.03) × $10^{-!}$	27	2570 (±28)
	0.2	8.68 (±0.94) × 10^{-2}	39	1741 (±144)
	0.1	1.37 (±0.04) × 10^{-1}	26	2601 (±79)

Table S5 Tabulated catalytic results for the recycling study of [*closo*-$B_{10}H_{10}$]$^{2-}$-decorated bimetallic Au_xAg_{1-x}NPs for 4-NP reduction, 5 mol% metal to 4-NP catalyst loading, after aging of the NPs for 1 d.

x	Cycle	k_{app} (s^{-1})	t_{rxn} (s)	TOF (h^{-1})
0.2	1st	9.45 × 10^{-2}	35	1968
	2nd	1.52 × 10^{-1}	21	3234
	3rd	9.92 × 10^{-2}	28	2429
	4th	7.64 × 10^{-2}	35	1946
	5th	3.06 × 10^{-2}	63	1081
	6th	6.38 × 10^{-2}	43	1593
0.6	1st	2.19 × 10^{-1}	20	3411
	2nd	2.08 × 10^{-1}	30	2307
	3rd	1.43 × 10^{-1}	41	1679
	4th	1.07 × 10^{-1}	55	1245
	5th	9.30 × 10^{-2}	67	1017
	6th	7.19 × 10^{-2}	80	851

Table S6 Tabulated catalytic results for the recycling study of [*closo*-$B_{10}H_{10}$]$^{2-}$-decorated bimetallic Au_xAg_{1-x}NPs for 4-NP reduction, 5 mol% metal to 4-NP catalyst loading, after aging of the NPs for 7 days.

x	Cycle	k_{app} (s^{-1})	t_{rxn} (s)	TOF (h^{-1})
0.2	1st	1.89×10^{-1}	20	3463
	2nd	1.64×10^{-1}	20	3345
	3rd	1.08×10^{-1}	27	2576
	4th	8.39×10^{-2}	30	2261
	5th	5.64×10^{-2}	49	1383
	6th	3.80×10^{-2}	55	1240
0.6	1st	7.31×10^{-2}	45	1525
	2nd	1.02×10^{-1}	30	2254
	3rd	5.89×10^{-2}	45	1505
	4th	2.41×10^{-2}	104	660
	5th	1.23×10^{-2}	186	367
	6th	7.67×10^{-3}	280	245

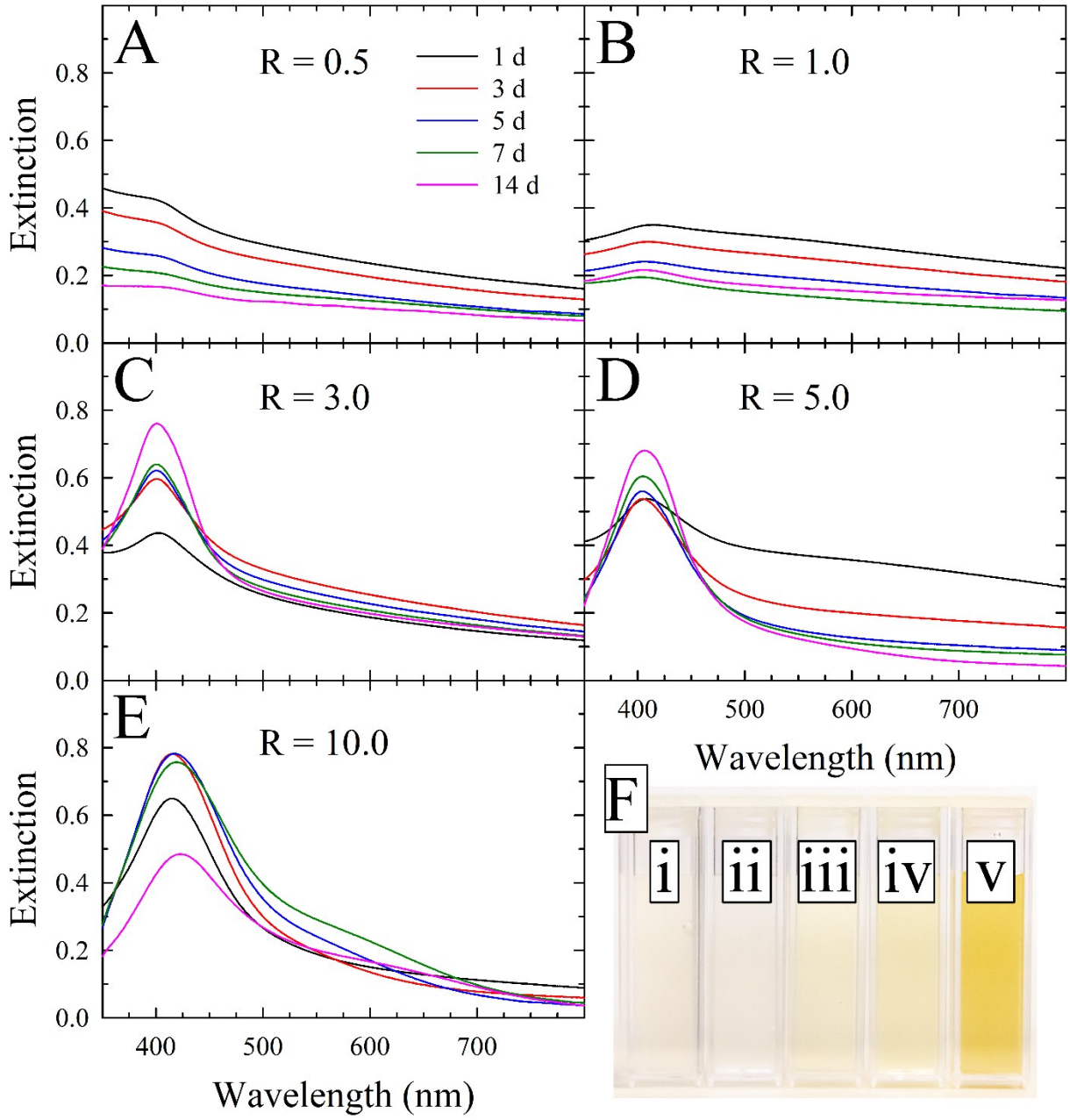

Fig. S1 Time-dependent UV–vis spectra for (A) R = 0.5, (B) R = 1.0, (C) R = 3.0, (D) R = 5.0, and (E) R = 10.0 [*closo*-$B_{10}H_{10}$]$^{2-}$-decorated **AgNPs**. Solutions prepared using R values less than 3.0 produced AgNPs with low LSPR bands and very little coloration as seen in panel F. Solutions prepared using R values greater than 1.0 exhibited ripening throughout the studied time frame. The legend in (A) applies to plots A–E. (F) Photograph of (left to right) R = 0.5, 1.0, 3.0, 5.0, 10.0 AgNPs, labelled numerically using Roman numerals, after aging for 3 days.

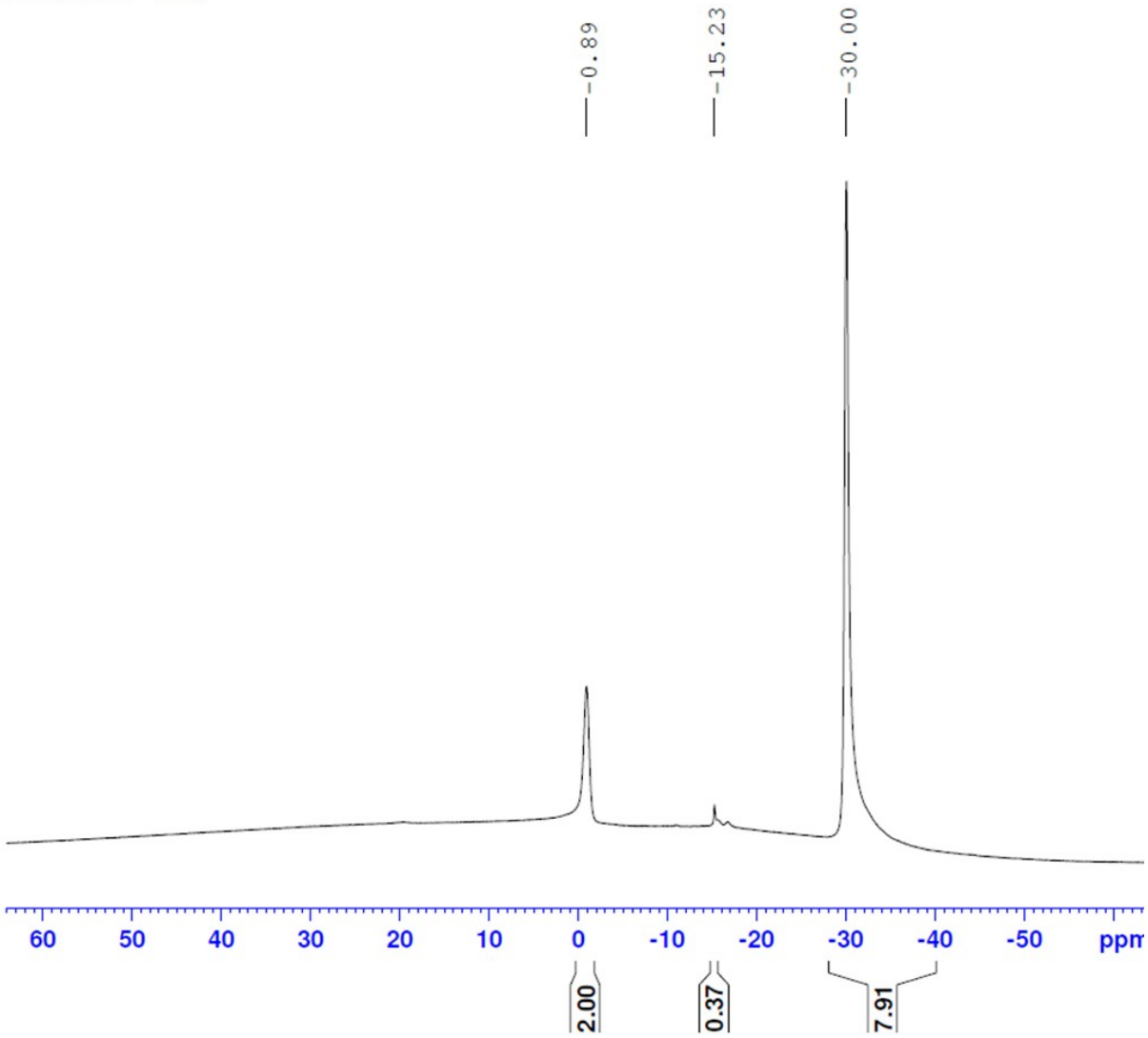

Fig. S2 Proton-decoupled ^{11}B-NMR spectrum of $Cs_2B_{10}H_{10}$; 400 MHz, H_2O, δ = –0.89 (apical B), –15.23 (residual [*closo*-$B_{12}H_{12}]^{2-}$), –30.00 (equatorial B).

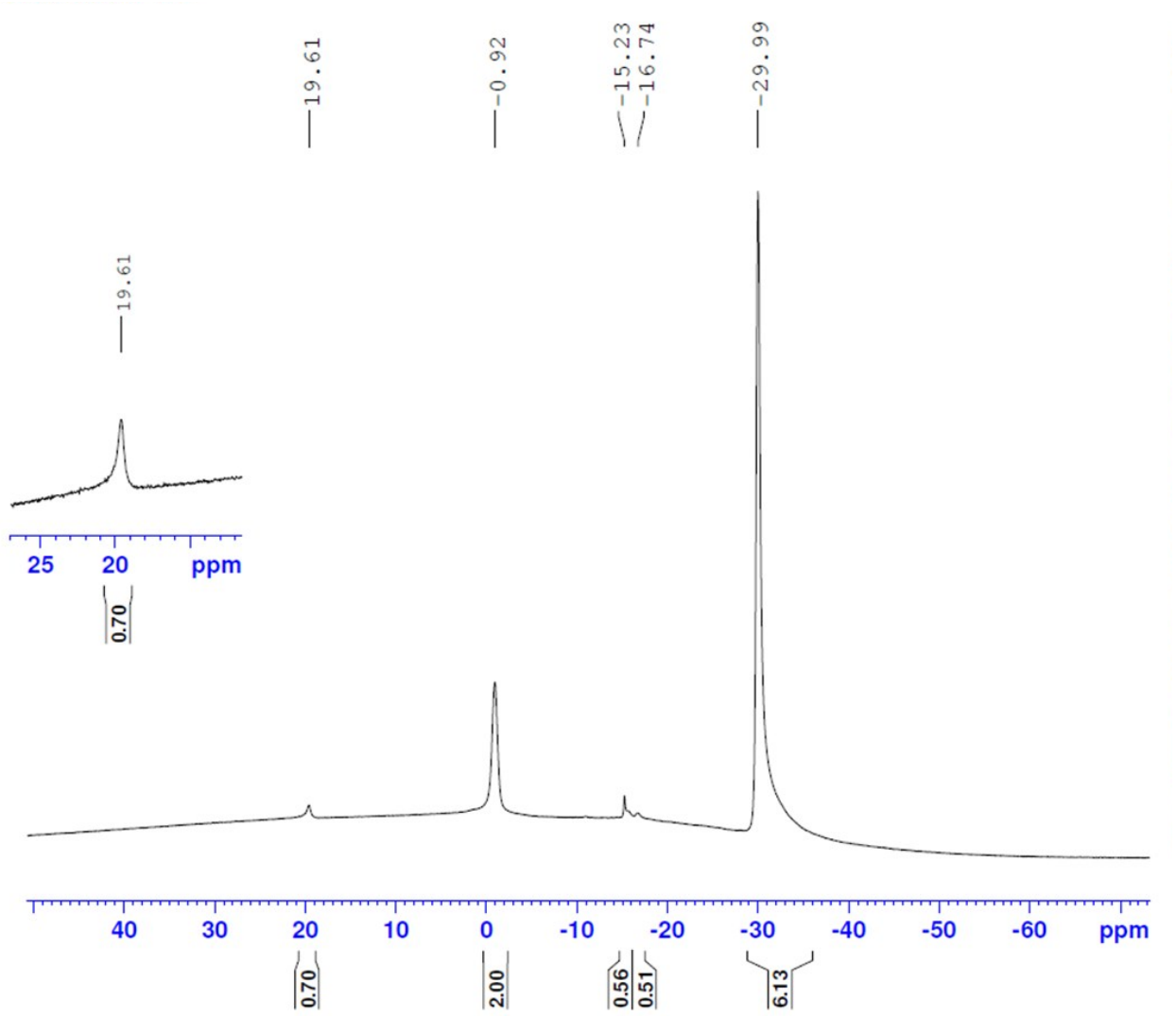

Fig. S3 Proton decoupled ^{11}B-NMR spectrum of colloidal [*closo*-$B_{10}H_{10}$]$^{2-}$-decorated AuNPs (R=10.0); 400 MHz, H_2O, δ = 19.61 (boric acid), –0.92 (apical B), –15.23 (residual [*closo*-$B_{12}H_{12}$]$^{2-}$), –29.99 (equatorial B).

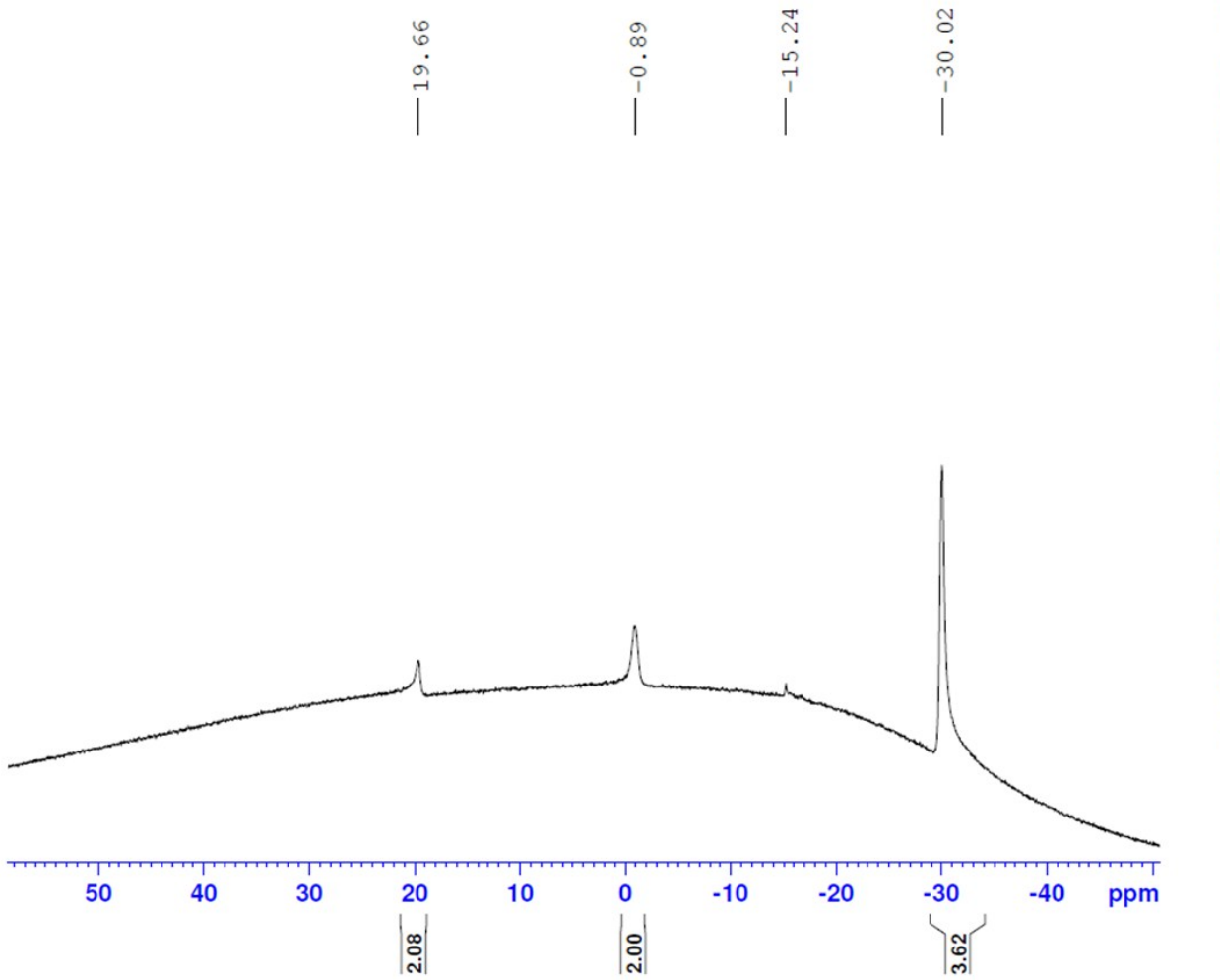

Fig. S4 Proton decoupled ^{11}B-NMR spectrum of colloidal [*closo*-$B_{10}H_{10}$]$^{2-}$-decorated AuNPs (R=1.0); 400 MHz, H_2O, δ = 19.66 (boric acid), –0.89 (apical B), –15.24 (residual [*closo*-$B_{12}H_{12}$]$^{2-}$), –30.02 (equatorial B).

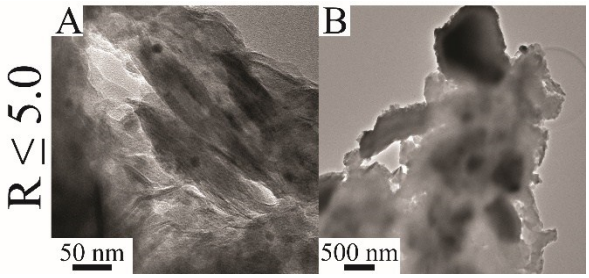

Fig. S5 Representative transmission electron microscopy (TEM) images representing [*closo*-$B_{10}H_{10}$]$^{2-}$-decorated **AgNPs** synthesized using an R value of 5.0 or less and aged for 3 days, resulting in aggregation upon drying on the TEM grid. The images in (A) and (B) represent solutions produced using R = 0.5 or R = 5.0, respectively.

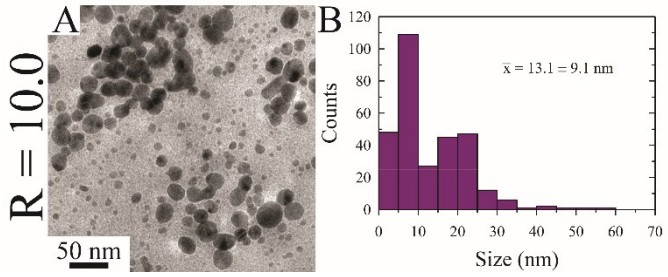

Fig. S6 (A) Representative TEM image and (B) corresponding histogram for [*closo*-$B_{10}H_{10}$]$^{2-}$-decorated **AgNPs** synthesized using an R value of 10.0 and aged for 3 days. The average particle size is greatly affected by the presence of many large aggregates amongst a population of smaller particles.

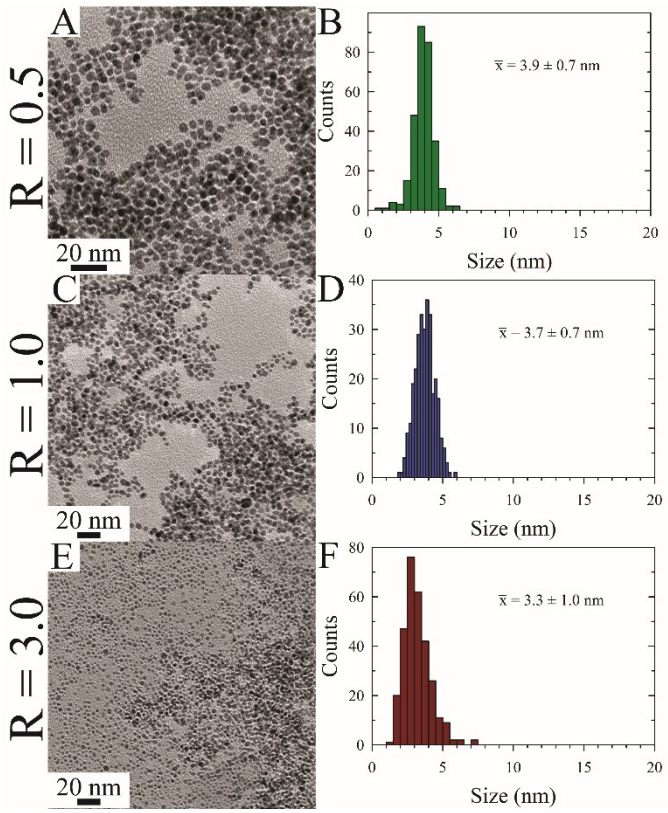

Fig. S7 (A, C, and E) Representative TEM images and (B, D, and F) corresponding histograms for [*closo*-$B_{10}H_{10}$]$^{2-}$-decorated **AuNPs** synthesized using R values of 0.5, 1.0, and 3.0 and aged for 3 days. While of the AuNPs produced in this study are quite small, images of the R = 3.0 sample present the smallest average size.

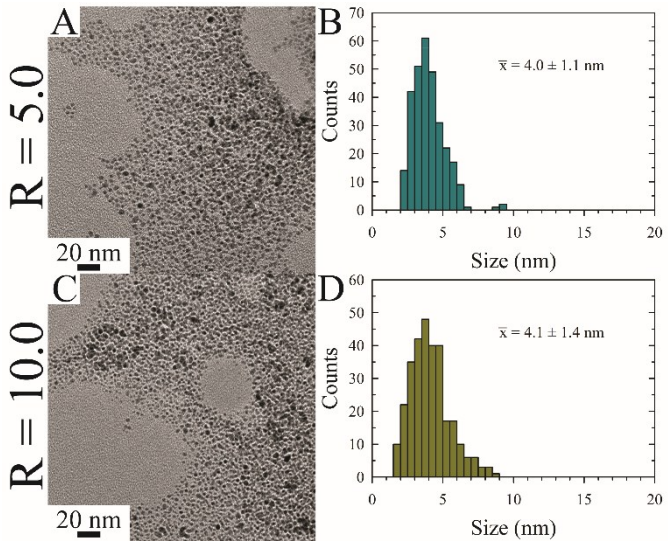

Fig. S8 (A and C) Representative TEM images and (B and D) corresponding histograms for [*closo*-$B_{10}H_{10}]^{2-}$-decorated AuNPs synthesized using a R values of 5.0 and 10.0 and aged for 3 days. While still small, the AuNPs represented here possess slightly larger average sizes. Notably, the R = 10.0 AuNP sample showed black aggregates once aged for 7 days.

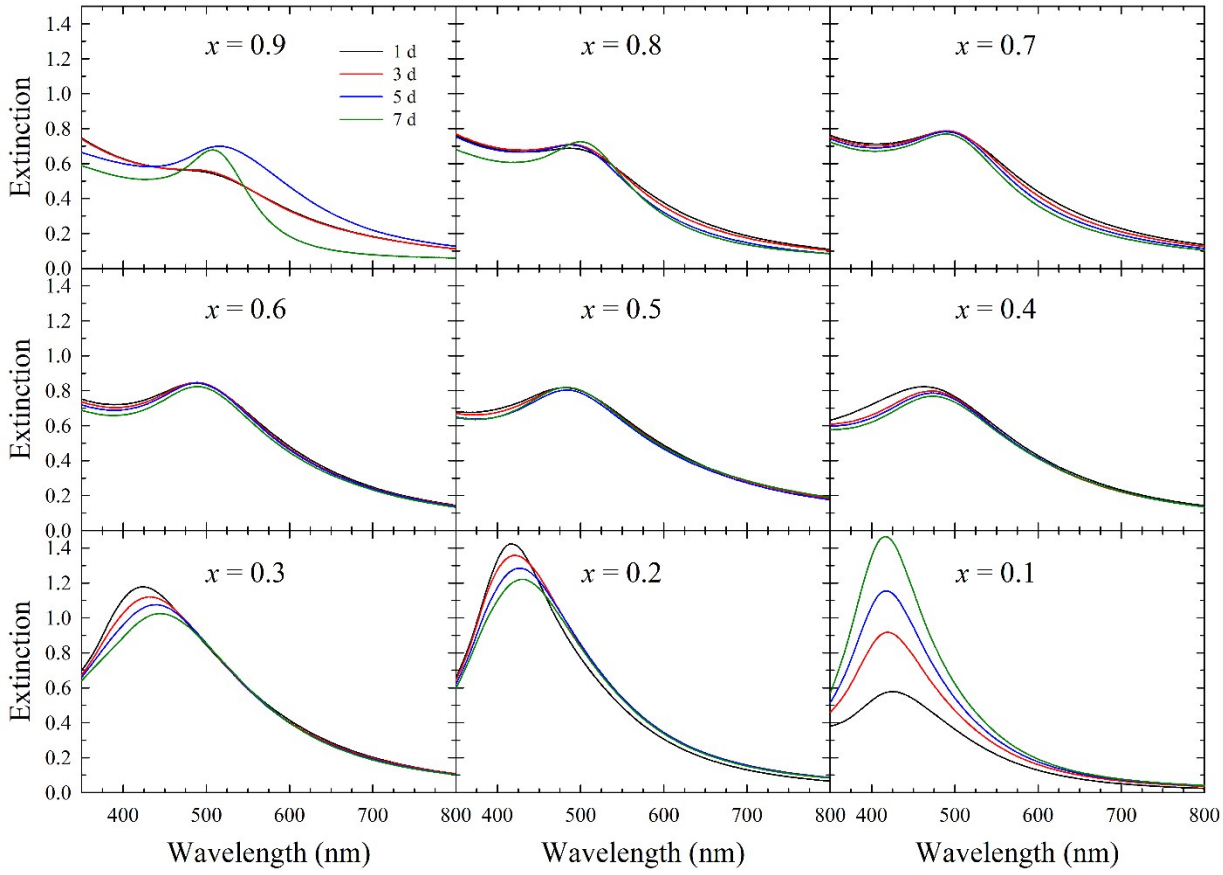

Fig. S9 UV–vis spectra of colloidal $B_{10}H_{10}^{2-}$-decorated bimetallic Au_xAg_{1-x}NPs synthesized using a reducing agent to metal molar ratio of 3.0 (R = 3.0). Stability measurements were acquired after aging for 1, 3, 5, and 7 days. The LSPR bands for x = 0.9, 0.3, 0.2, and 0.1 all undergo dramatic shifts as the NPs ripen over time, similar to the changes undergone for the monometallic Au- and AgNPs. The legend in the first plot (for *x* = 0.9) applies to all other plots.

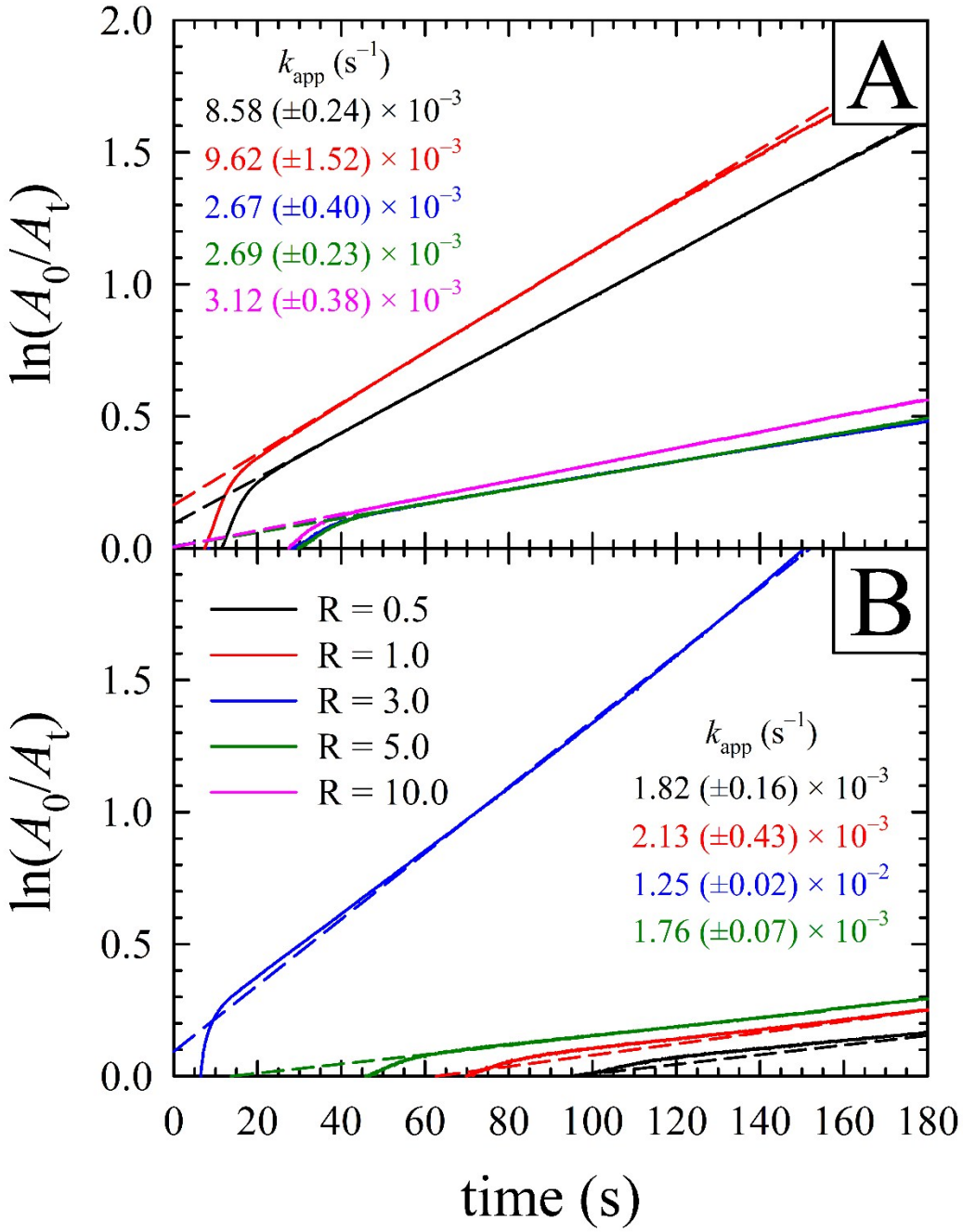

Fig. S10 Catalyzed reduction of 4-NP to 4-AP by $NaBH_4$ when using [*closo*-$B_{10}H_{10}$]$^{2-}$-decorated AuNPs aged for (A) 1 day and (B) 7 days as catalysts. The dashed lines show the linear portion of each rate plot. Aging appears to have a mixed effect on the apparent catalytic rate (k_{app}), with AuNPs produced using R = 0.5, 1.0, and 5.0 showing significant drops in activity while R = 3.0 shows a dramatic increase in activity after aging. The R = 10 sample showed black precipitate after aging for 7 days, and as such the aged sample was ignored for this study. Catalyst loading was 5 mol% Au to 4-NP in all cases. The legend in (B) applies to both plots.

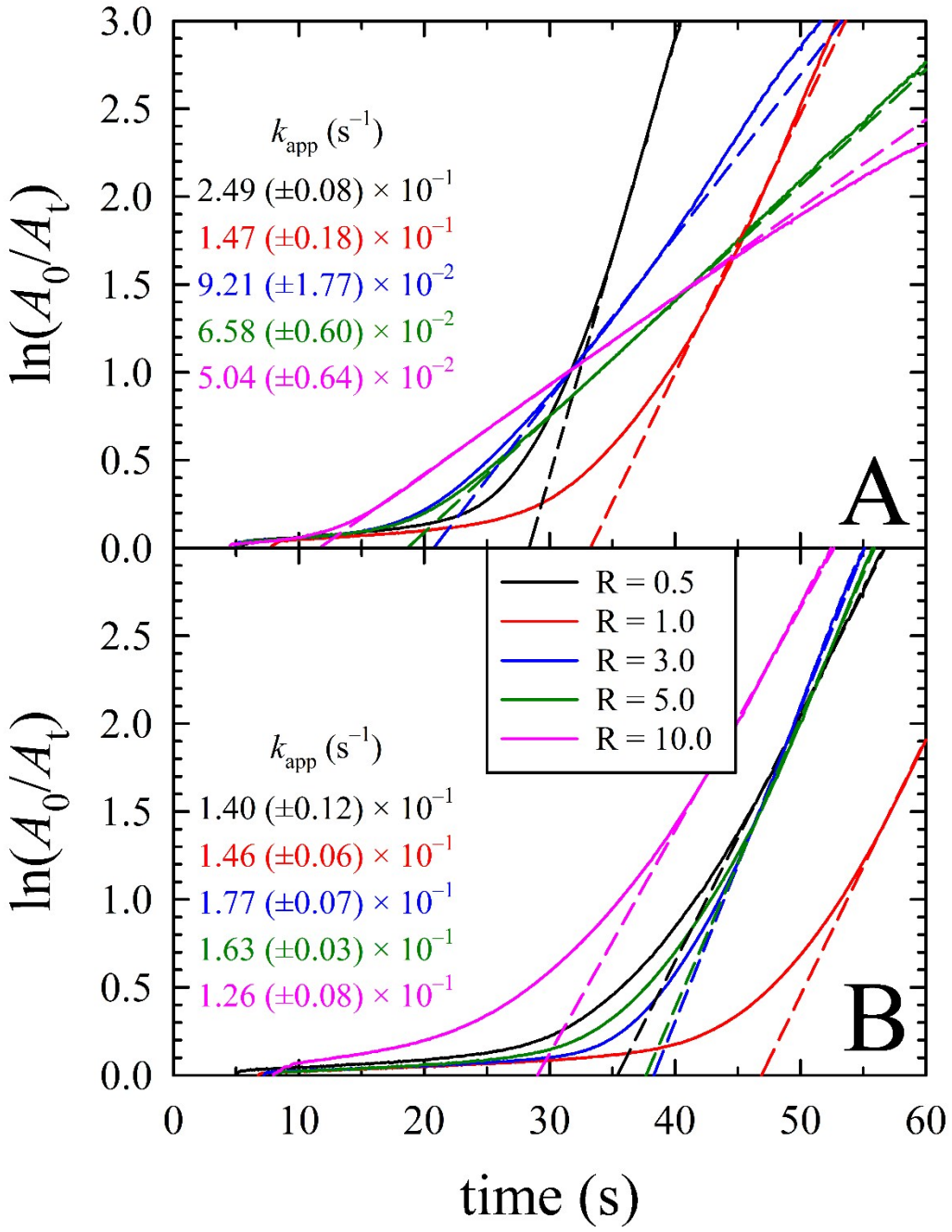

Fig. S11 Catalyzed reduction of 4-NP to 4-AP by $NaBH_4$ when using [*closo*-$B_{10}H_{10}$]$^{2-}$-decorated AgNPs aged for (A) 1 day and (B) 7 days as catalysts. The dashed lines show the linear portion of each rate plot. Upon aging, the apparent catalytic rate (k_{app}) for AgNPs produced using R = 0.5 decreased while those for AgNPs produced using R = 3.0, 5.0, and 10.0 increased dramatically. The k_{app} of the R = 1.0 sample showed negligible change upon aging for 7 days. Catalyst loading was 5 mol% Ag to 4-NP in all cases. The legend in (B) applies to both plots.

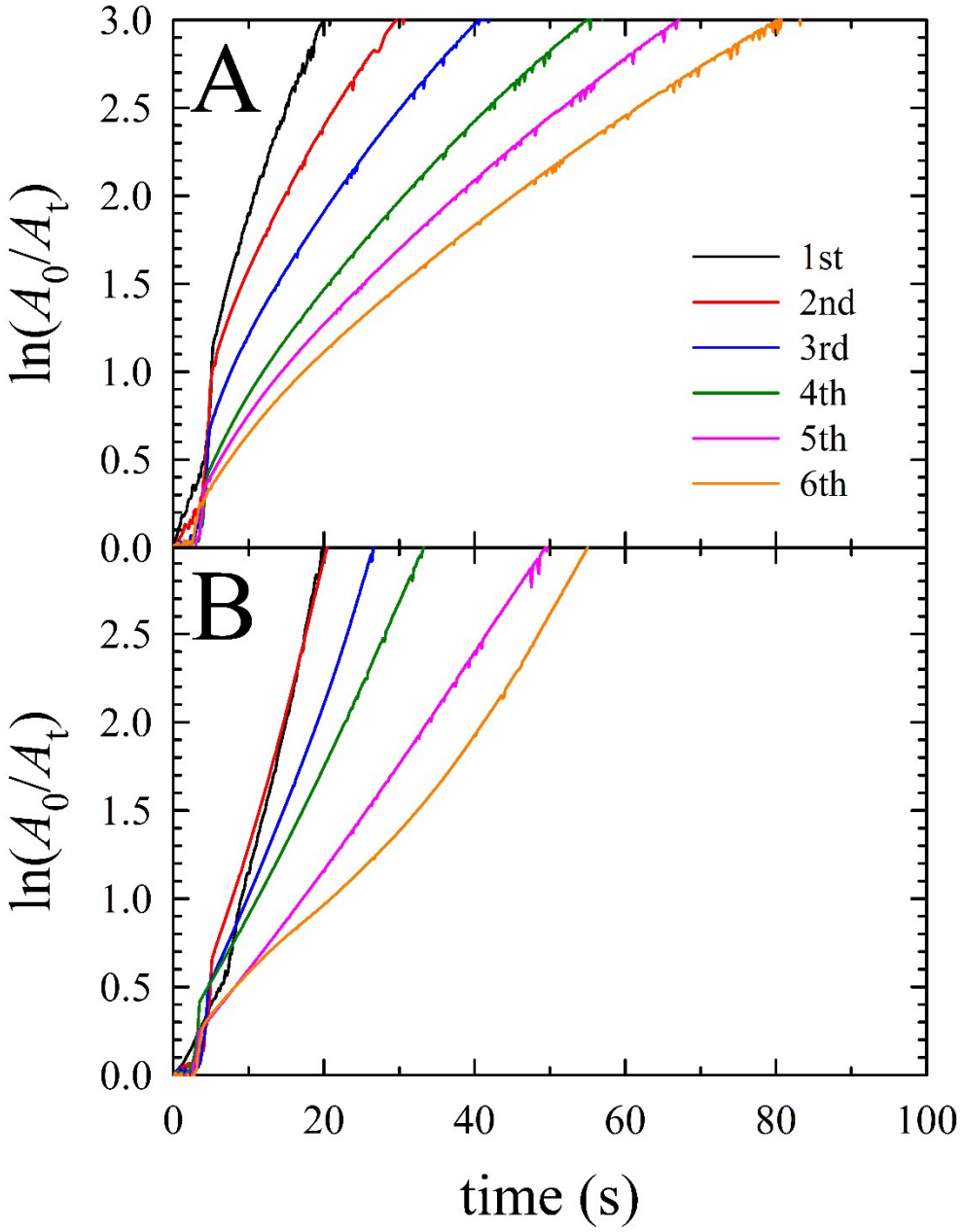

Fig. S12 Recycling study for 4-NP reduction to 4-AP when using [*closo*-$B_{10}H_{10}$]$^{2-}$-decorated Au_xAg_{1-x}NPs aged for (A) 1 day and (B) 7 days, where x = 0.6. The legend indicates the reduction cycle. These NPs show poor recyclability, herein attributed to poisoning of the NP surface with excess borohydride and reaction products.

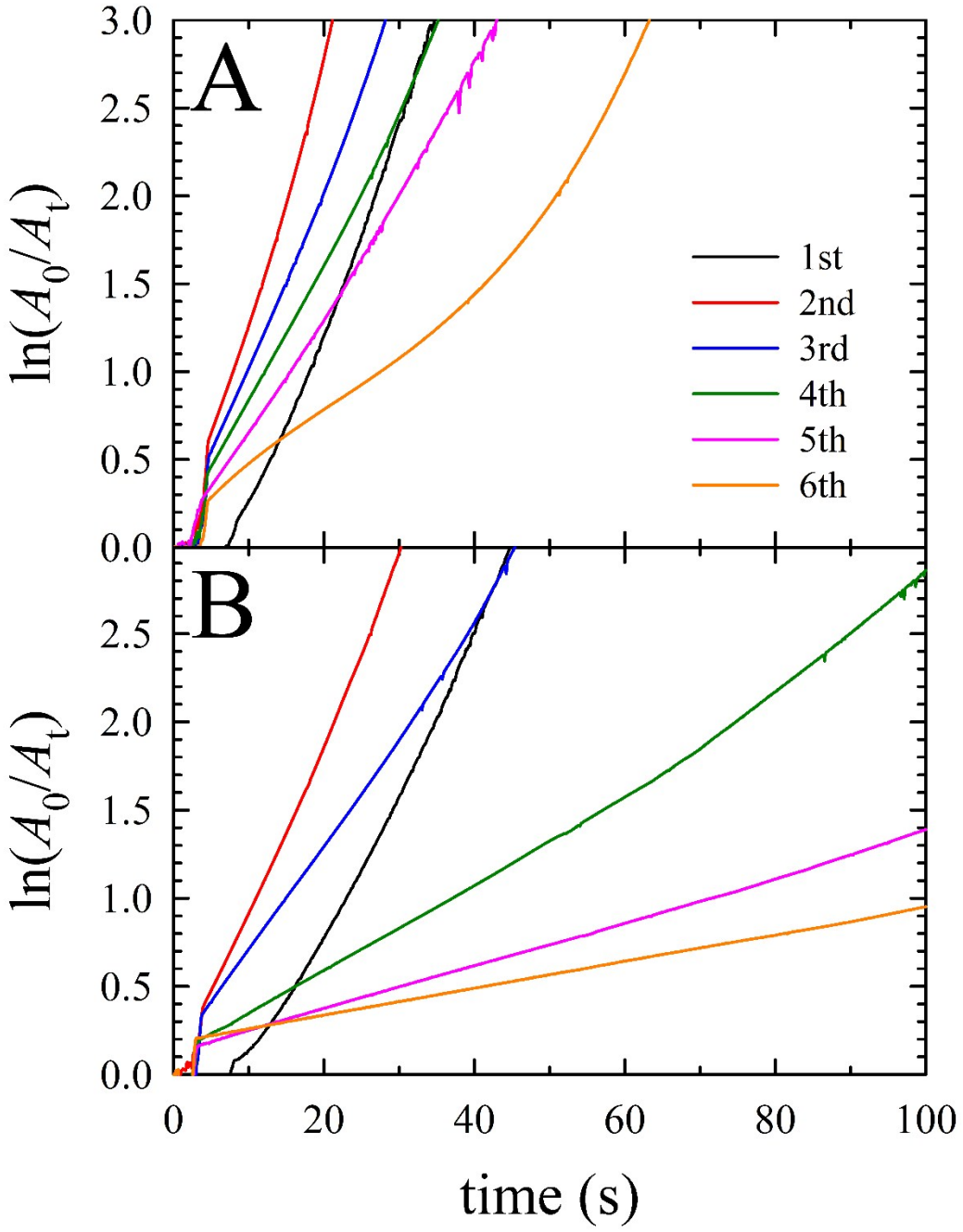

Fig. S13 Recycling study for 4-NP reduction to 4-AP when using [*closo*-$B_{10}H_{10}$]$^{2-}$-decorated Au_xAg_{1-x}NPs aged for (A) 1 day and (B) 7 days, where x = 0.2. The legend indicates the reduction cycle. These NPs show poor recyclability, herein attributed to poisoning of the NP surface with excess borohydride and the reaction products.

1. Hawthorne, F. M.; Pilling, R. L.; Knoth, W. H., Bis(Triethylammonium) Decahydrodecaborate(2−). In *Inorganic Syntheses*, Tyree Jr., S. Y., Ed. 1967.